

Characterization and genomic profiling of potential iron-reducing bacteria isolated from red mud for bioremediation

Akhmad Subkhan¹, Ainul Fitria Mahmudah², Shintawati³, Widi Astuti⁴,
Himawan Tri Bayu Murti Petrus^{5,6}, Matin Nuhamunada¹, Yekti Asih Purwestri^{1,2*}

¹ Department of Tropical Biology, Faculty of Biology, Universitas Gadjah Mada, Yogyakarta, Indonesia

² Research Center for Biotechnology, Universitas Gadjah Mada, Yogyakarta, Indonesia

³ Industrial Chemical Engineering Technology Study Program, Department of Agricultural Technology, Politeknik Negeri Lampung (Polinela), Jln. Soekarno – Hatta Nomor: 10, Rajabasa Raya, Bandar Lampung, Lampung, Indonesia

⁴ Research Center for Mineral Technology, National Research and Innovation Agency (BRIN), Jl. Ir. Sutami Km. 15, Tanjung Bintang 35361, Indonesia

⁵ Department of Chemical Engineering, Sustainable Mineral Processing Research Group, Faculty of Engineering, Universitas Gadjah Mada, Jl. Grafika No. 2, Kampus UGM, Yogyakarta 55281, Indonesia

⁶ Unconventional Geo-Resources Research Center, Faculty of Engineering, Jl. Grafika No. 2, Kampus UGM, Yogyakarta 55281, Indonesia

* Corresponding author's e-mail: yekti@ugm.ac.id

ABSTRACT

Red mud is waste from the alumina (Al_2O_3) production process of bauxite ore processing through the bayer process. The production of one ton of alumina produces between 1–1.5 tons of red mud. The high amount of waste has a negative impact on the environment, resulting in infertile soil and posing long-term human health risk. The content of ferric oxide (Fe_2O_3) as the main mineral in red mud is promising to be reused as a first step in waste handling. This study aims to isolate and identify Fe-reducing bacteria from red sludge waste and find out what genes and compounds are likely to be involved in the process. A 5 g sample of red mud was put into physiological solution for dilution and then cultured in MHA media containing 50 mg/L ferrous ammonium sulfate (FAS). There were 16 isolates that grew and was then analyzed using repetitive PCR. Different isolates were then screened for reduction tests using ferrozine reagent on MHA+ Fe_2O_3 50 mg/L media and obtained 7 potential Fe-reducing isolates. Further tests were carried out on liquid media to determine the OD of Fe^{2+} and cells measured at 562 and 600 nm wavelengths at 0, 12 and 24 hours. Identification of Fe metal reducing bacteria using 16S rRNA gene and nucleotide sequence alignment using BioEdit software while WGS analysis was annotated using BV-BRC with RASTtk pipeline, BlastKoala, genome mining of secondary metabolites using AntiSMASH and type (strain) genome server (TYGS) to show the results of phylogenetic analysis. The results of this study found the presence of 7 bacterial isolates with different species capable of reducing Fe metal from red mud including *Kytococcus sedentarius* (As 1), Order of *Staphylococcus arlettae* (As 3), *Halalkalibacterium halodurans* strain (As 6), *Halalkalibacterium halodurans* strain (As 8), *Bacillus paranthracis* (Ai 3), *Stutzerimonas stutzeri* (Ai 7) and *Cytobacillus firmus* (Ai 8). *Bacillus paranthracis* (Ai 3) confirmed the possibility that its compounds and genes can be involved in the metal reduction process.

Keywords: red mud, reduction, 16S rRNA, repetitive-PCR, whole genome sequencing, metallophore, bacillibactin.

INTRODUCTION

Red mud (RM) is a solid waste generated during the processing of bauxite ore through the Bayer process to produce alumina (Al_2O_3). The production of one ton of alumina can generate

approximately 1–1.5 tons of red mud (Liu and Naidu, 2014). Notably, one of the companies in Indonesia responsible for a substantial amount of red mud production is PT Indonesia chemical alumina (ICA) in west Kalimantan. ICA processes bauxite ore into chemical grade alumina

(CGA) with an annual production capacity of 300,000 tons of CGA and an output of approximately 600,000 tons of red mud each year (Yao et al., 2023). Improper disposal of red mud can have detrimental effects on soil fertility and disrupt natural habitat (Viljoen et al., 2022). The alkalinity of red mud typically ranges from pH 11–13 (Reddy and Rao, 2018), and the high ionic strength it contains poses long-term environmental risks and health hazards to humans (Kotnala et al., 2022).

To mitigate the negative impact of red mud waste, it can be repurposed for further processing. Red mud contains a significant amount of ferric oxide (Fe_2O_3) as its primary mineral, comprising approximately 44.3% of its composition (Sarath and Krishnaiah, 2022). Utilizing this ferric oxide (Fe_2O_3) can serve as an initial step in waste management, allowing for the creation of zero-valent iron. The highest reactivity synthesizing zero-valent iron is achieved when the iron (Fe) element is in the Fe^{3+} form, thus necessitating the reduction of Fe^{2+} in red mud first. While various extraction methods have been explored using a comprehensive approach, employing a biological approach represents a more environmentally friendly alternative that has yet to be extensively studied.

Iron (Fe) plays a pivotal role in biogeochemical cycles as the most abundant redox active metal in the Earth's crust. It is an essential micronutrient required by nearly all living organisms, participating in Fe redox reaction (He et al., 2021). Leveraging the potential Fe-reducing microbes can help minimize the environmental impacts associated with chemical processes. Iron reducing bacteria (IRB) are instrumental in biogeochemical processes that occur through the anaerobic respiration of Fe^{3+} oxides (Li et al., 2022). These bacteria have the capacity to convert ferric ions (Fe^{3+}) into ferrous ions (Fe^{2+}) (Matus et al., 2019). Harnessing indigenous bacteria from the local environment is particularly beneficial as they possess a specific metabolism suited to their surroundings. Therefore, to initiate waste management and enhance the utilization of red mud, it is imperative to isolate and identify Fe-reducing bacteria from this waste material.

In an effort to better understand the mechanism of iron reduction by bacteria, whole genome sequencing (WGS) analysis is a very important tool. WGS allows the identification of genes and metabolic pathways that play a role in the iron

reduction process, including enzymes involved in electron transfer as well as regulatory factors that affect reduction efficiency. By uncovering the genetic composition of iron-reducing microbes, this study can provide insight into the broader biotechnological potential of red mud utilization, including applications in bioremediation and recovery of valuable metals. Through this approach, this study seeks to not only identify microbial species that have iron reduction capabilities, but also understand the molecular mechanisms underlying their activities under extreme environmental conditions such as red mud.

MATERIALS AND METHODS

Bacterial isolation from Red Mud

Red Mud samples were each taken in quantities of 1 g subsequently subjected to serial dilution using an 8.5% NaCl solution. These diluted samples were then introduced into petri dishes containing MHA media, adjusted to a pH of 10 and enriched with Ferrous Ammonium Sulphate (FAS) at a concentration of 50 mg/L. The petri dishes were incubated at a temperature of 30 °C for 48 hours. The growing bacterial colonies were taken for purification. Purification was carried out using the streak plate method onto new MHA media that has been added with 50 mg/L FAS iron media, then incubated at 30 °C for 48 hours.

Bacterial DNA isolation and initial screening

Bacterial isolates were grown onto 50 mg/L MHB+FAS medium and incubated for 48 hours at 30 °C. Bacterial DNA isolation refers to the method stated in the Geneaid DNA Isolation Kit. The DNA obtained was used for the initial screening. Initial screening of various bacterial isolates isolated from red mud, the rep-PCR method was used, using BOX A1R primers ('5-TAC GGC AAG GCG ACG CTG ACG-3'). This was done to eliminate the same type of bacteria through the bands formed for further testing.

Screening Fe-reducing bacteria

Screening of potential Fe-reducing bacteria was carried out using MHA media that had been added with Fe_2O_3 iron at a concentration of 50 mg/L. The bacterial isolates that had been purified

were then grown on the media using the streak plate method. After that, it was incubated in an incubator at 30 °C for 24 hours. Fe reduction by potential bacteria was confirmed using the ferrozine reagent by dripping it onto bacterial isolates that grew on the media. A positive result was indicated by a magenta color change in the ferrozine droplets. The method was adapted from Schalk et al. (2021) with modifications.

Bacterial characterization and identification

Characterizing potential Fe-reducing bacteria involved comprehensively examining their morphology and physiology using gram staining, endospore staining, motility testing and catalase testing. Genomic DNA was extracted using a bacterial DNA kit (Geneaid) for molecular identification. Subsequently, PCR amplification was carried out with universal primers 27F (5'-AGTTTGATCCTGGCTCAG-3') and 1492R (5'-GGTTACCTTGTTACGACTT-3'). The obtained DNA sequences were subjected to BLAST analysis utilizing the NCBI database (<http://www.ncbi.nlm.nih.gov>).

Assessment of bacterial Fe reduction potential

To evaluate the potential of bacteria for Fe reduction, the following protocol was employed: MHB media was used at a concentration of 21 g/L. To this media, HEPES buffer (4.76 g/L) and an iron source in the form of Fe₂O₃ (50 mg/L) were added (Ghorbanzadeh et al., 2014). In the logarithmic growth phase, bacteria are characterized by an OD of 0.5 (H. Li et al., 2022). To determine Fe²⁺ reduction, ferrozine reagent (1 mL/25 mL of the sample) was added immediately before analyzing in the spectrophotometer. Subsequently, the sample was incubated for 5 minutes, with a positive result indicated by the emergence of a magenta color. The OD value of Fe²⁺ was measured at a wavelength of 562 nm (Ghorbanzadeh et al., 2014) and the OD value of bacteria was assessed at 600 nm using UV-visible spectrophotometry. These measurements were taken at 12 and 24 hours, respectively. The reduction test was conducted in an Erlenmeyer flask, covered with dark plastic and incubated using a shaker incubator at 30 °C.

Whole genome sequencing of bacterial Fe reduction

Bacterial genome isolation was performed by taking 5 ml of bacterial culture and centrifuging it in a 1.5 ml tube to obtain a bacterial pellet. Genomic DNA was extracted using the ZymoBIOMICS™ DNA Miniprep Kit, and the quality and concentration were assessed using NanoDrop. Genome bacteria was sequenced using a nanopore sequencing. Briefly, the long-read library was prepared using a Ligation Sequencing gDNA-Native Barcoding Kit 24 V14 (SQK-NBD114,24) (Oxford Nanopore Technologies, Oxford, UK) and sequenced on Promethion P24, 10.4.1 flow cell (Oxford Nanopore Technologies, Oxford, UK). Base calling, quality control, and adapter trimming were performed using Dorado basecaller model dna_r10.4.1_e8.2_400bps_sup@v4.3.0 (Oxford Nanopore Technologies, Oxford, UK).

Bioinformatic analyses were performed on the assembled genome to assess functional annotation, taxonomic classification, and secondary metabolite biosynthetic potential. Genome statistics, coding sequence predictions, and subsystem classifications were obtained via the Bacterial and Viral Bioinformatics Resource Center (BV-BRC) (<https://www.bv-brc.org/app/Annotation>). Functional gene annotation was conducted using BLAST Koala (KEGG Automatic Annotation Server) (<https://www.kegg.jp/blastkoala/>). Whole-genome-based phylogenetic analysis was carried out using the Type (Strain) Genome Server (TYGS) (<https://tygs.dsmz.de/>) to determine taxonomic placement and evolutionary relationships. Furthermore, biosynthetic gene clusters (BGCs) related to secondary metabolite production were predicted using AntiSMASH (<https://antismash.secondarymetabolites.org/>).

RESULT AND DISCUSSION

Isolation of potential Fe-reducing bacteria from Red Mud

The main objective of this study was to isolate bacteria from red mud waste that can potentially reduce Fe metal. A total of 16 isolates isolated from red mud were able to grow on FAS iron-enriched MHA media with a pH of 10. Bacterial differences were obtained based on colony morphology observed from shape, elevation, margin, surface, and color. The isolation of

Fe-reducing bacteria in this study involved using red mud waste samples from aluminum processing, which exhibited a pH range of 10–11. pH measurements served as a reference for formulating bacterial growth media. It is well-established that bacterial growth can be influenced by various factors, including biotic factors such as the organisms in an ecosystem and abiotic factors such as pH, temperature, and salinity. The 16 isolates obtained were then screened using rep-PCR. Rep-PCR is used to compare genetic kinship in bacterial isolates by looking at the band pattern formed on the electrophoresis gel as a result of amplifying noncoding regions between repetitive elements (Spinler et al., 2022). Rep-PCR was performed using BOX A1R primers to see kinship and confirm differences between isolates. The BOX-PCR method is a molecular fingerprinting method useful for grouping bacteria with similar genetic kinship (Poonchareon et al., 2019). In the BOX element, there is a repetitive element consisting of a combination of three subunit sequences including BOXA, BOXB and BOXC which have a length of 59, 45 and 50 nucleotides respectively (Bilung et al., 2018).

The results of rep-PCR visualization in the form of bands from the 16 bacterial isolates can be seen in Figure 1. These results show that each bacterial isolate has a different band pattern from each other, so it is known that the bacterial isolates obtained previously based on differences in colony morphology have differences from each other. The bands formed by electrophoresis were then further analyzed using PyElph 1.4 software. The software determines the band's position formed from the rep-PCR results and creates a dendrogram (Nikolić et al., 2018). The results

of band analysis using PyElph 1.4 software were carried out for bacterial grouping using the unweighted pair group method and arithmetic mean (UPGMA) method in the software to determine the relationship between isolates in the form of a dendrogram (Figure 1b.). Based on the analysis dendrogram analysis in Figure 1b. with a similarity value of 40% imaginary lines are made to touch the dendrogram lines of all isolates. These results indicate that the isolates obtained are different, with a similarity value of 40%.

Screening Fe-reducing bacteria

Bacterial isolates were tested using MHA media with 50 mg/L Fe_2O_3 iron concentration as a substrate to be reduced by bacteria. 16 bacterial isolates that were able to grow on MHA media containing Fe_2O_3 (50 mg/L) were screened to obtain potential bacteria capable of reducing Fe_2O_3 . The test uses a ferrozine indicator by adding a few drops around the bacterial colonies that grow on the media. Positive results of the reduction test are characterized by a change in color to magenta (purple) in the media and around the growing bacterial colonies as in Figure 2. The color change that occurs around bacterial colonies and media when ferrozine is added indicates a reduction process carried out by bacteria. Ferrozine reagent will form a complex bond with divalent iron characterized by a magenta (purple) color produced by the reaction (Mandal & Sen, 2018; Smith et al., 2021). Seven of the sixteen bacterial isolates that have been tested can reduce Fe_2O_3 (Figure 2). In the environment, bacteria have different physiological mechanisms. Some bacteria can utilize substrates in the environment to carry out metabolic

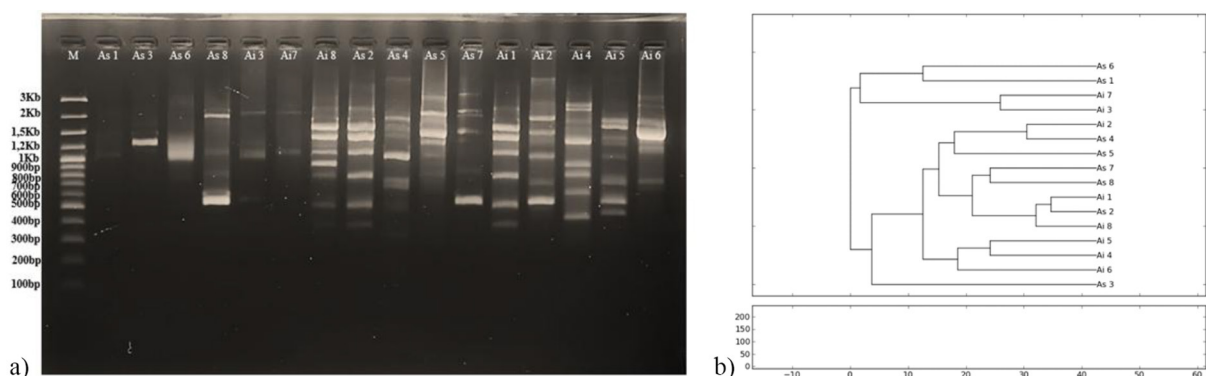


Figure 1. (a) Rep-PCR analysis revealed distinct band patterns among the sixteenth bacterial isolates obtained from red mud, indicating species-level differences between each isolate, (b) the bands formed by electrophoresis were then further analyzed using PyElph 1.4 software

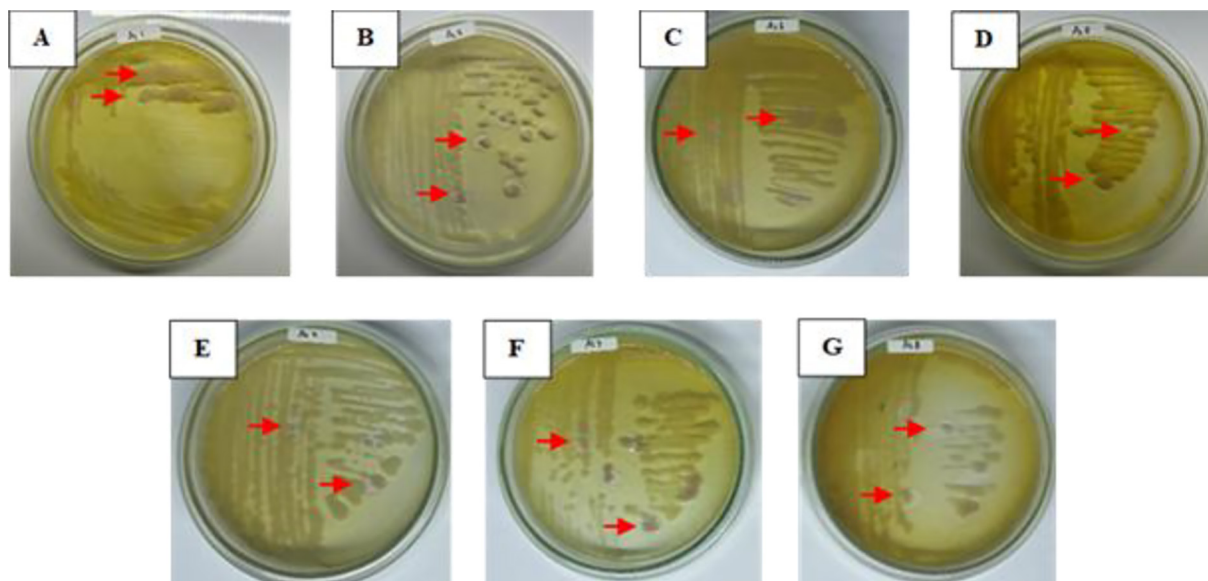


Figure 2. Potential bacterial isolates demonstrating Fe_2O_3 reduction are identified by a distinct color change to purple upon the addition of ferrozine (indicated by arrows) in the isolated codes: As 1 (A); As 3 (B); As 6 (C); As 8 (D); Ai 3 (E); Ai 7 (F); Ai 8 (G). This color shift is attributed to the presence of Fe^{2+} reduction products interacting with ferrozine in the media

activities and produce metabolites (Dong et al., 2023). In the red mud waste environment, there are various chemicals and metals including SiO_2 , Al_2O_3 , Fe_2O_3 , MgO , CaO , K_2O , SO_3 , Na_2O , and TiO_2 (Kang & Kim, 2023). This content will affect the metabolism of bacteria that grow.

The results of bacterial isolation from red mud contained bacteria that can reduce Fe metal. Some genera of bacteria can reduce include *Thiobacillus*, *Anaeromyxobacter*, *Geobacter* and *Geobacillus* (Yao et al., 2023). In addition, some bacteria can produce redox reactions both directly and indirectly, such as the species *Acidithiobacillus ferrooxidans* (At.f.) and *Thiobacillus thiooxidans* (T.f.) (Dong et al., 2023). Other bacteria that are capable of reducing Fe (III) metal includes *Shewanella* sp, *Albidoferax ferrireducens*, and *Geothrix fermentans* (Kappler et al., 2021). Potential bacterial isolates that can be reduced are then tested using MHB liquid media that has been added with Fe_2O_3 iron (50 mg/L).

Assessment of bacterial Fe reduction potential

Potential bacterial isolates that can be reduced are then tested using MHB liquid media that has been added with Fe_2O_3 iron (50 mg/L). Testing using liquid media to determine the concentration of Fe^{2+} resulting from the reduction process. Fe^{2+} concentration was obtained from the OD

measurement using a spectrophotometer. Measurements were made using a ferrozine reagent indicator. Tests using ferrozine have been widely carried out to determine the presence of iron ions from various samples such as minerals and biology (Smith et al., 2021). Ferrozine will react with divalent iron in the sample to form a magenta-colored complex bond that is soluble in water, the color complex is measured using a wavelength of 562 to determine the OD value of Fe^{2+} formed (Balamurugan et al., 2019).

In addition to measuring the OD of Fe^{2+} , the OD of bacteria was measured, this is to determine the relationship between bacterial growth and the Fe^{3+} reduction process. The resulting data shows the relationship between bacterial growth and the Fe^{3+} reduction process, the higher the OD of bacteria is directly proportional to the higher OD value of Fe^{2+} obtained (Figure 3). This can occur due to the reduction process carried out by all test bacterial isolates as a catalytic agent. All bacteria are able to grow and develop in media containing Fe_2O_3 , confirmed by the increase in OD that has been measured at hours 0, 12 and 24 (Figure 3). Reduction activity in all isolates can be due to all bacteria having reductase enzymes. It has been widely known that bacterial species have iron reductase enzyme activity from proteins in the cytoplasmic membrane (Cain and Smith, 2021). Based on the data presented in Figure 3, the highest activity of Fe^{3+} reduction to Fe^{2+} was observed

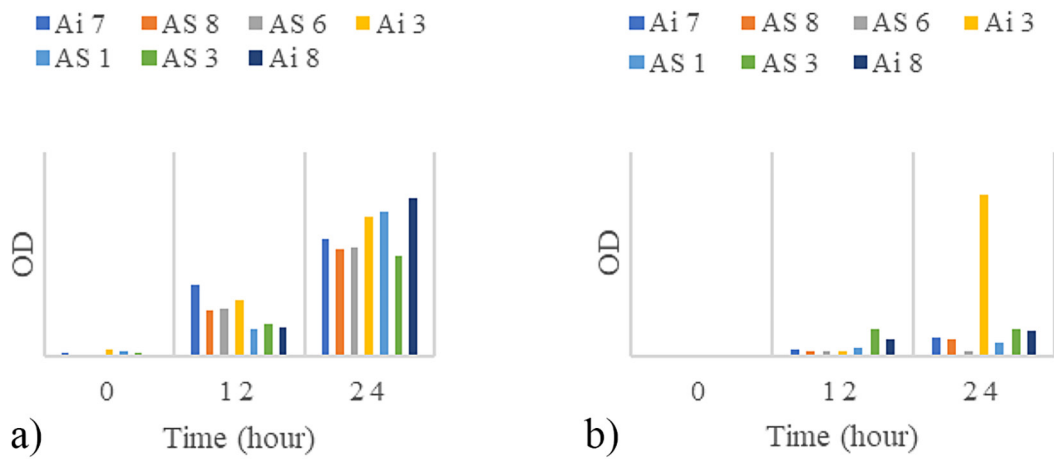


Figure 3. The Fe³⁺ reduction activity to Fe²⁺ of potential bacteria was assessed through measurement of A. OD of bacteria (600 nm) and B. OD Fe²⁺ (562 nm). The graph demonstrates an increase in both bacterial growth and Fe²⁺ concentration

in isolate Ai 3. This activity is likely influenced by the bacterium’s ability to produce secondary metabolites that act as metal-chelating agents from the surrounding environment. In addition, specific genes involved in the reduction process may also play a significant role. To confirm the relationship between the genetic potential and the metabolites produced, whole genome sequencing (WGS) analysis was performed on isolate Ai 3.

Bacterial characterization and identification

Colony morphology characteristics are often used to complement conventional microbial identification data to determine the diversity between bacterial strains (Sousa et al., 2013). Based on Table 1, it shows that the bacterial isolates taken have differences in colony morphological characteristics both in shape, elevation, margin, colony surface and color. The difference in these characteristics

indicates that the 7 isolates of potential Fe-reducing bacteria obtained from the isolation and purification results are of different types.

The results of bacterial isolation were confirmed through cell morphology and molecular characteristics to determine that the isolates taken differed. In addition to observing colony morphology, cell observations were made in the form of gram staining and endospore staining. Gram and endospore staining are very important because it is done to determine the characteristics of bacteria and make it easier to know the shape of bacterial cells during observation under a microscope. Gram staining is a common technique in distinguishing types of bacteria based on their cell walls. Gram-negative (–) bacteria are characterized by pink cells while gram-positive (+) are characterized by purple. The results of observations made by the seven bacterial isolates capable of reducing Fe showed purple and pink

Table 1. Observation of cell morphology, chemical tests and bacterial motility

No.	Isolate code	Cell Morphology			Catalase	Motility
		Shape	Gram	Endospore		
1	As 1	Coccus	+	-	+	-
2	As 3	Coccus	+	-	+	-
3	As 6	Bacillus (<i>Streptobacillus</i>)	+	+	+	+
4	As 8	Bacillus (<i>Streptobacillus</i>)	+	+	+	+
5	Ai 3	Bacillus (<i>Streptobacillus</i>)	+	+	+	+
6	Ai 7	Bacillus	-	-	+	+
7	Ai 8	Bacillus	+	-	+	+

colors (Figure 4). The purple color produced from crystal violet contains large molecules that cannot penetrate into the peptidoglycan layer of the positive bacterial cell wall, thus producing a purple color (Vigneshwaran et al., 2020).

Gram-positive bacteria obtained from red mud waste are related to the survival mechanism of these bacteria, both physically and chemically. The cell wall of gram-positive bacteria has a dense wall structure so that the bacteria can survive the pressure of the external environment (Cheng et al., 2023). The cell wall structure of gram-positive bacteria has peptidoglycan with a thickness of about 20–80 nm (Vigneshwaran et al., 2020). Red mud waste is an extreme environment, has high alkalinity and contains several metals such as SiO_2 , CaO , Al_2O_3 and Fe_2O_3 (Li et al., 2023), therefore the growing bacteria have their mechanism for survival. Gram-positive bacteria have the ability to take iron sources

through membrane-anchored binding proteins and are transported intracellularly through ATP-binding cassettes on the membrane (Liu et al., 2023). Gram-positive bacteria that are known to be able to reduce Fe are *B. cereus* and *S. aureus* (Jing et al., 2022). The adaptation mechanism of gram-negative bacteria is the presence of bacterial membrane proteins consisting of membrane fusion protein (MFP) and outer membrane factor protein (OMF) which function to transport heavy metals, proteins, and other compounds from the cytoplasmic membrane and cellular accumulation in the environment (Mathivanan et al., 2021). Previous research has known that gram-negative bacteria strain *Pseudomonas* sp. B50D has the ability to remove mercury metal (Giovannella et al., 2017).

Endospore staining uses malachite green and safranin dyes. Through the heating process, malachite green dye will penetrate into the endospore

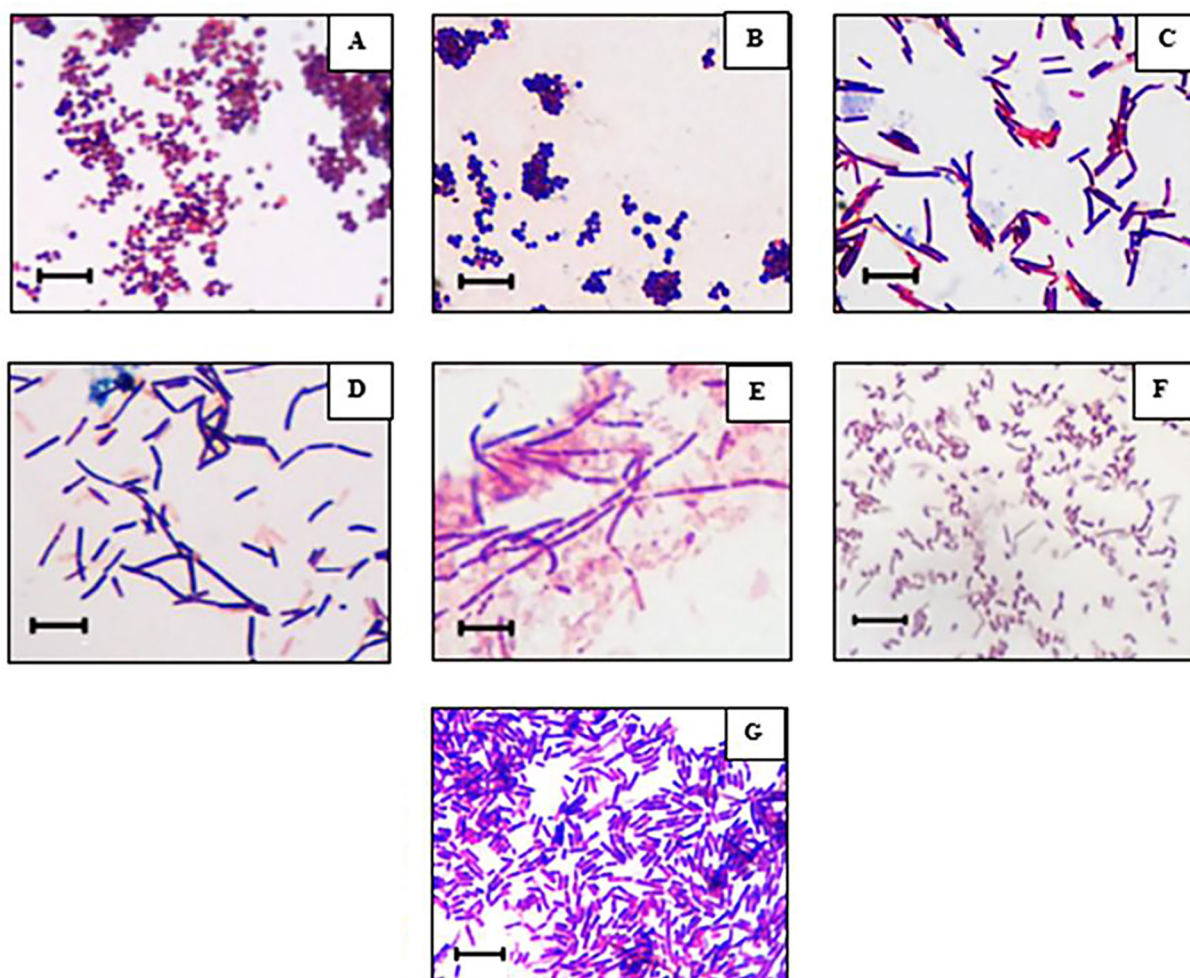


Figure 4. Results of gram staining of Fe metal reduction potential bacterial cells, gram negative bacteria such as isolate code As 1 (A); As 3 (B); As 6 (C); As 8 (D); Ai 3 (E); Ai 8 (G) and negative bacteria isolate code Ai 7 (F) with 100x magnification. Bar: 5 μm

which gives a green color to the bacterial spores, while safranin gives a red color to the bacterial vegetative cells. The seven potential bacterial isolates with Fe metal reduction potential include three isolates with endospores, including As 6, As 8, and Ai 3. (Figure 5 and Table 1). The presence of endospores in bacteria is a form of bacterial adaptation in unfavorable conditions and will develop when environmental conditions return to normal or favorable (Awasti & Anand, 2022). Bacterial endospores can withstand high temperatures, UV radiation, drought, and chemical or enzymatic treatments. This defense mechanism is related to the condition of red mud waste which has a fairly high pH, which is around 10–11, besides that, there are still many metal contents present in the waste.

The results of biochemical activity tests on all potential bacterial isolates that reduce Fe metal is able to produce catalase enzyme. Positive results of the catalase test are characterized by the presence of bubbles when the bacterial isolate is tested with H_2O_2 (hydrogen peroxide) (Figure 6). According to Man et al., (2022), catalase is an enzyme capable of decomposing hydrogen peroxide (H_2O_2) as a specific substrate into oxygen (O_2) and water (H_2O). The role of the catalase enzyme in bacteria is used as a form of self-defense in the face of oxidative stress. This mechanism is related to the origin of bacteria being isolated from red mud waste which has high metal content. Metal toxicity can affect metabolic conditions in bacteria that can stimulate the formation of ROS and inactivate enzymes (Sazykin and Sazykina, 2023).

Motility tests were carried out on all isolates of potential Fe-reducing bacteria. This is to determine whether there is mobility carried out by the bacteria. This is needed to determine other characteristics of bacteria in understanding chemotaxis, biofilm formation and virulence (Casado-García et al., 2021). The motility test uses semi-solid

media. Positive motile tests are characterized by the spread of bacteria on semi-solid media after incubation, while negative motility bacteria only grow on the former ose needle puncture. Bacteria can move by using their means of movement such as flagellum by rotating them, therefore the bacteria are able to shift in media with lower agar content (Casado-García et al., 2021). The motility test shows that of the seven isolates, there are two isolates with negative motility, namely isolates As 1 and As 3 (Table 1).

Molecular characteristics are used to identify bacterial isolates capable of reducing Fe metal using the 16S rRNA gene from selected isolates namely As 1, As 3, As 6, As 8, Ai 3, Ai 7 and Ai 8. Bacterial DNA is used as a template in the amplification process with PCR. The amplification process uses universal primers namely 27F and 1492R. The use of the 16S rRNA gene in this identification is because the gene is found in all bacteria and is a common target for identification (El-Liethy et al., 2023). The gene is highly conserved which consists of nine hypervariable domains separated by fragments (Rossi-Tamisi-er et al., 2015). The use of 16S sequences to distinguish strains based on polymorphisms in the gene (Johnson et al., 2019). The 16S rRNA PCR results that have been carried out on the seven bacterial DNA samples capable of reducing Fe metal show the results of the amplicons size of 1,500 bp (Figure 7). These results show that the target gene for bacterial identification has met the requirements. According to Algarni, (2022) amplification using universal primers will produce an amplicon size of about 1,500 bp. The sequence analysis process uses Nucleotide BLAST on the website www.ncbi.nih.gov to determine the similarity of isolate nucleotide sequences with other bacteria in the GenBank database. The results of the Nucleotide BLAST analysis are description, scientific name, max score, total

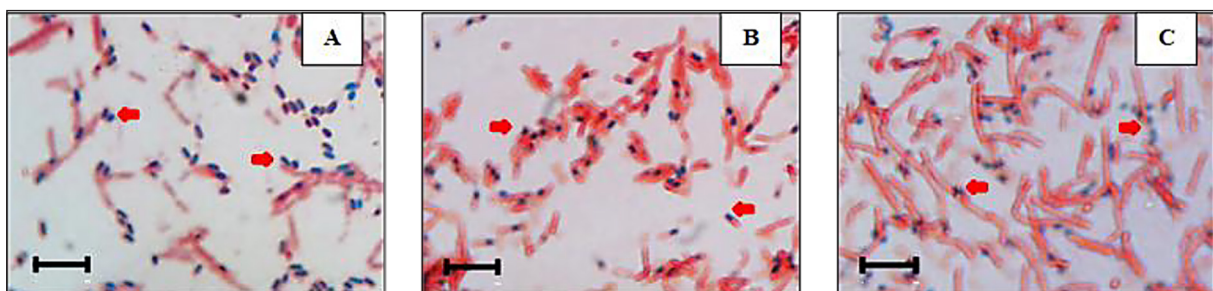


Figure 5. Observation of bacterial cell endospores on isolate codes As 6(A); As 8(B); Ai 3(C) with 100x magnification. Detection of dark green endospores (red arrow) Bar: 5 μ m

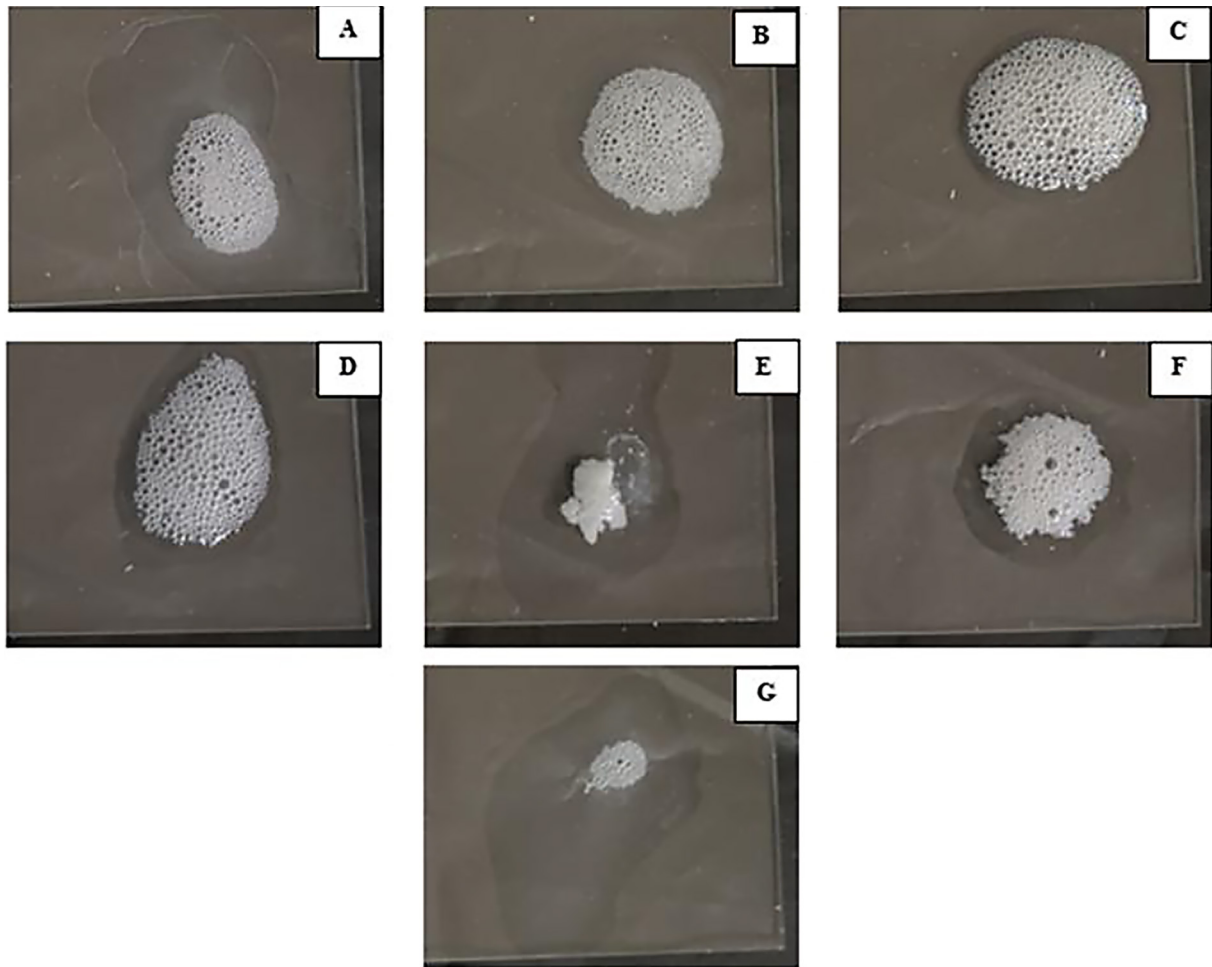


Figure 6. Catalase test results on isolates As 1 (A); As 3 (B); As 6 (C); As 8 (D); Ai 3 (E); Ai 7 (F); Ai 8 (G). Positive results of the catalase test are characterized by the presence of bubbles when the bacterial isolate is dripped with H_2O_2



Figure 7. 16S rRNA gene amplification results using primers 27F and 1492R. M (Marker 100 bp-3,000 bp)

score, percentage of query coverage, E-value, percentage identity, and accession number.

The results for the strains most similar to the isolate are presented in Table 2. These findings are based on sequence analysis using BLAST. Isolate similarity is assessed using the query coverage and percentage identity values. According to Newell et al. (2013), query coverage refers to the percentage of the nucleotide sequence that aligns with database sequences during the BLAST process. A higher query coverage generally results in a lower E-value. Percentage identity values greater than 95% typically indicate genus-level similarity, while values above 97% suggest species-level similarity (Johnson et al., 2019). Isolate AS 1 is identified as *Kytococcus sedentarius*, a Gram-positive coccus (Sims et al., 2009). It does not form endospores, is catalase-positive, and is non-motile (Lim et al., 2021). Previous studies have shown that *Kytococcus sedentarius* can produce keratinase enzymes (Kee et al., 2021; Kotala et al., 2022) and degrade diphenylarsinic acid compounds (Nakamiya et al., 2007). Isolates AS 6 and AS 8, based on BLAST results are identified as *Halalkalibacterium halodurans* (Table 2). This species is a homotypic synonym of *Bacillus halodurans*, as recognized by the International Code of Nomenclature of Prokaryotes (ICNP). A homotypic synonym refers to different names for the same type strain (Madhaiyan et al., 2020). *Bacillus halodurans* is a Gram-positive bacterium, typically forms irregularly shaped white colonies, and is catalase-positive (Kunal et al., 2016). Research has shown that this species can reduce alkalinity and heavy metal concentrations (Kaur et al., 2022).

Isolate Ai 7 corresponds to *Stutzerimonas stutzeri*, a homotypic synonym of *Pseudomonas stutzeri*, also recognized by the ICNP. *Pseudomonas stutzeri* has been reported to reduce hexavalent chromium (Sathishkumar et al., 2017). Isolate Ai 8 is identified as *Cytobacillus firmus*,

which has a synonymous name, *Bacillus firmus* (Dong et al., 2023). Previous observations have shown that this bacterium is Gram-positive, catalase-positive, and motile. It forms colonies with rhizoid edges and raised elevations, similar to the characteristics described by Rao and Narasu (2007). *Bacillus firmus* is known for its ability to reduce chromium (Sau et al., 2010). Isolate AS 3 shows genetic relatedness to *Staphylococcus arlettae* ATCC 43957, with a percentage identity of only 85.93%. Species are considered to be in the same family when the percentage identity exceeds 86.5% (Hitch et al., 2021), in the same order when > 82.0%, in the same class when > 78.5%, and in the same phylum when > 75.0% (Yuan et al., 2021). Therefore, isolate AS 3 belongs to the same order as *Staphylococcus arlettae*, namely Caryophanales. Prior research has shown that *S. arlettae* can reduce chromium (Sagar et al., 2012). Isolate Ai 3, based on sequence analysis, shows similarity to *Bacillus paramycooides* strain MCCC 1A04098, with a percentage identity of 84.09%. This value suggests that isolate AI 3 shares similarity at the order level with *B. paramycooides*, which also belongs to the order Caryophanales.

Whole genome sequencing analysis of bacterial isolate Ai 3

Isolate Ai 3 was analyzed using WGS to identify genes associated with bacterial-metal interactions in the environment, including genes responsible for metal reduction. Additionally, the analysis aimed to uncover secondary metabolites involved in metal utilization processes. The Comprehensive Genome Analysis service provided a fully assembled genome, with annotated features summarized in Table 3 and Figure 8. The results revealed that the genome of isolate Ai 3 has a total length of 5,513,510 base pairs (bp), consisting of four contigs. The largest contig, which accounts for half of

Table 2. Results of homologous species

No	Isolate	Homologous Species	Query cover	Per. Ident	E value	Accession number
1	As 1	<i>Kytococcus sedentarius</i> DSM 20547	100%	97.99%	0.0	NR_074714.2
2	As 6	<i>Halalkalibacterium halodurans</i> DSM 497	100%	98.14%	0.0	NR_025446.1
3	As 8	<i>Halalkalibacterium halodurans</i> DSM 497	100%	97.94%	0.0	NR_025446.1
4	Ai 7	<i>Stutzerimonas stutzeri</i> CCUG 11256	100%	98.26%	0.0	NR_118798.1
5	Ai 8	<i>Cytobacillus firmus</i> NBRC 15306	97%	98.07%	0.0	NR_112635.1
6	As 3	<i>Staphylococcus arlettae</i> ATCC 43957	97%	85.93%	0.0	NR_024664.1
7	Ai 3	<i>Bacillus paramycooides</i> MCCC 1A04098	100%	84.09%	0.0	NR_157734.1

Table 3. Genome assembly and annotation of *Bacillus paranthracis* (Isolate Ai 3)

Genome statistics	
Contigs	4
Genome length	5515310
GC content	35.471733
Contig L50	1
Contig N50	5174835
Annotation statistics	
tRNA	115
rRNA	45
CDS	5645
CDS ratio	1.0235145
Hypothetical CDS	1318
Hypothetical CDS ratio	0.38441098
PLFAM CDS	5486
PLFAM CDS ratio	0.97183347
Genome quality	
Coarse consistency	99.7
Fine consistency	98.5
CheckM completeness	100
Genome quality	Good

the total genome, had an N50 value of 5,174,835 bp (Table 3). A phylogenetic tree was also constructed to determine the taxonomic placement of the isolate. Using the Type (Strain) Genome Server (TYGS), phylogenetic analysis showed that isolate Ai 3 is closely related to *Bacillus paranthracis*

MCCC 1A00395, with strong bootstrap support of 93. A bootstrap value ≥ 90 indicates a highly reliable and strongly supported phylogenetic relationship (Aman et al., 2025).

Color coding in the TYGS phylogenetic output reflects differences in genome size, number of proteins, and species/subspecies clusters. Isolate Ai 3 shares the same color as *Bacillus paranthracis* MCCC 1A00395, confirming that both belong to the same phylogenetic cluster (Figure 9). Therefore, it can be concluded that isolate Ai 3 is *Bacillus paranthracis*. These results differ from the initial 16S rRNA analysis, where isolate AI 3 showed only 84.09% identity, a value insufficient for species-level identification. As such, WGS data is essential for confirming species identity, as it provides comprehensive genomic information, including more accurate insights into phylogenetics and taxonomy (Kislichkina et al., 2024).

AntiSMASH analysis of the *Bacillus paranthracis* genome was performed to predict secondary metabolites potentially involved in metal utilization in environmental contexts. As shown in Table 4, the analysis identified several biosynthetic gene clusters (BGCs) responsible for producing secondary metabolites. Notably, one of the predicted clusters encodes a Non-Ribosomal Peptide (NRP) metallophore, which shares 85% similarity with the known compound Bacilibactin, according to the antiSMASH database. NRP-type metallophores are synthesized

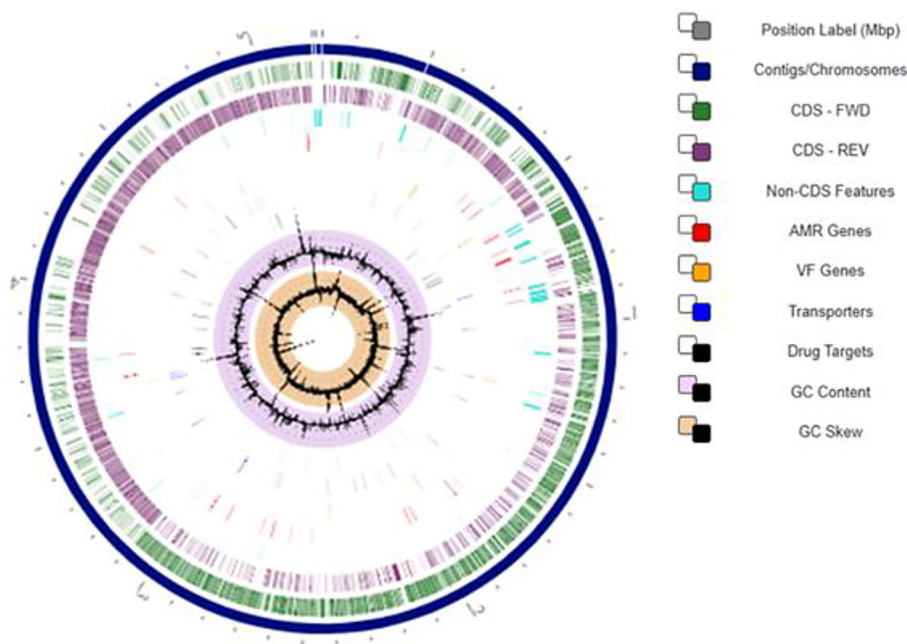


Figure 8. A circular graphical display of the distribution of the genome annotations for *Bacillus paranthracis*

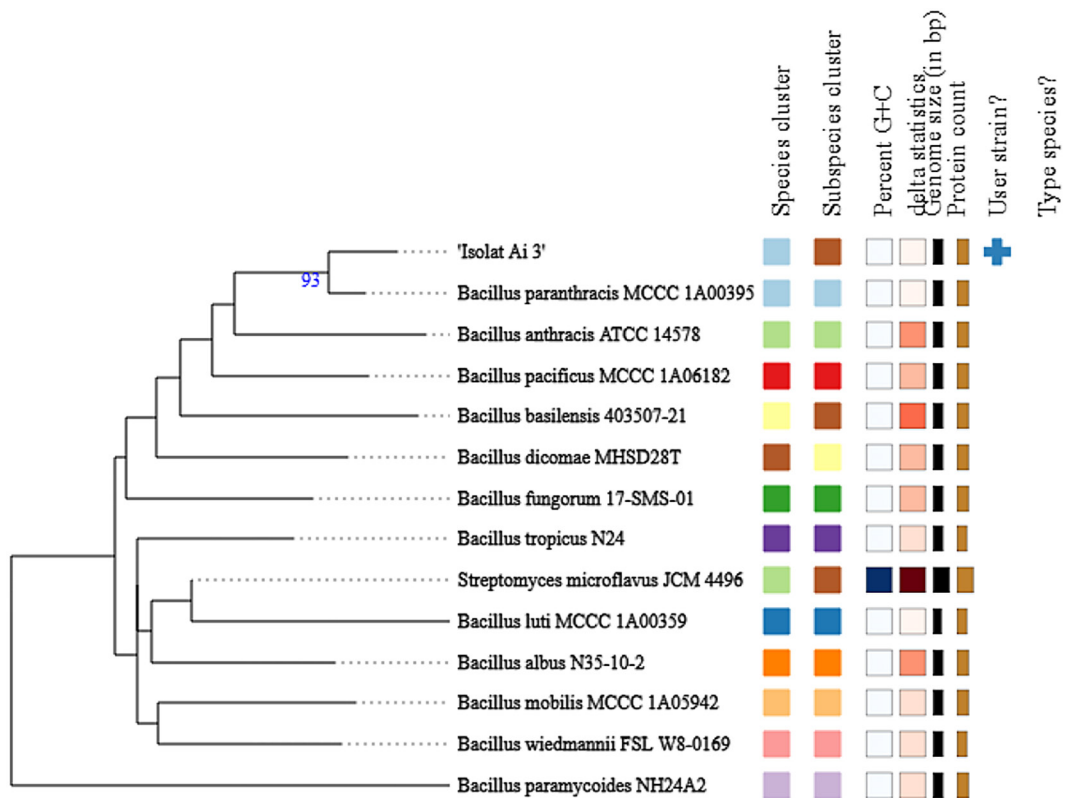


Figure 9. Result of phylogenetic tree construction from isolate Ai 3 genome using Type (Strain) Genome Server. The results showed that the isolate is a *Bacillus paranthracis*

Table 4. List of the putative gene clusters encoding for secondary metabolites by antiSMASH analysis in *Bacillus paranthracis* genome

Region	Type	From	To	Most similar known cluster	Similarity
Region 1.1	Arylpolyene,NRPS	240,512	302,062	-	-
Region 2.1	Lanthipeptide-class-ii	204,158	227,316	Cerecidin	RiPP: Lanthipeptide 94%
Region 2.2	LAP	1,835,493	1,858,999	-	-
Region 2.3	NRP-metallophore, NRPS	2,804,461	2,856,187	Bacillibactin	NRP 85%
Region 2.4	Betalactone	2,954,271	2,979,509	Fengycin	NRP 40%
Region 2.5	RiPP-like	3,079,828	3,090,094	-	-
Region 2.6	Terpene	3,842,389	3,864,242	Molybdenum cofactor	Other 17%
Region 2.7	Lasso peptide	3,988,821	4,012,745	Paeninodin	RiPP 100%
Region 2.8	RiPP-like	4,916,548	4,928,764	-	-

independently of ribosomes and play a critical role in metal binding. These compounds are secreted by microorganisms to chelate specific metals from the environment, enhancing their availability for biological processes (Luo et al., 2024). Additionally, metallophore production serves as a resistance mechanism in metal-rich environments (Gomes et al., 2024). Given that *Bacillus paranthracis* was isolated from red mud waste, a metal-rich industrial byproduct, the presence of

these genes supports the bacterium’s adaptation to such environments through metallophore-mediated chelation.

According to antiSMASH genome analysis, the gene cluster encoding the NRP-metallophore is located at positions 2,804,461 to 2,856,187 nt, spanning 51,727 nucleotides (Figure 10). This cluster shows 100% similarity with the NRP-metallophore gene cluster from *Bacillus cereus* strain 7/27/S131 and 95% similarity with other

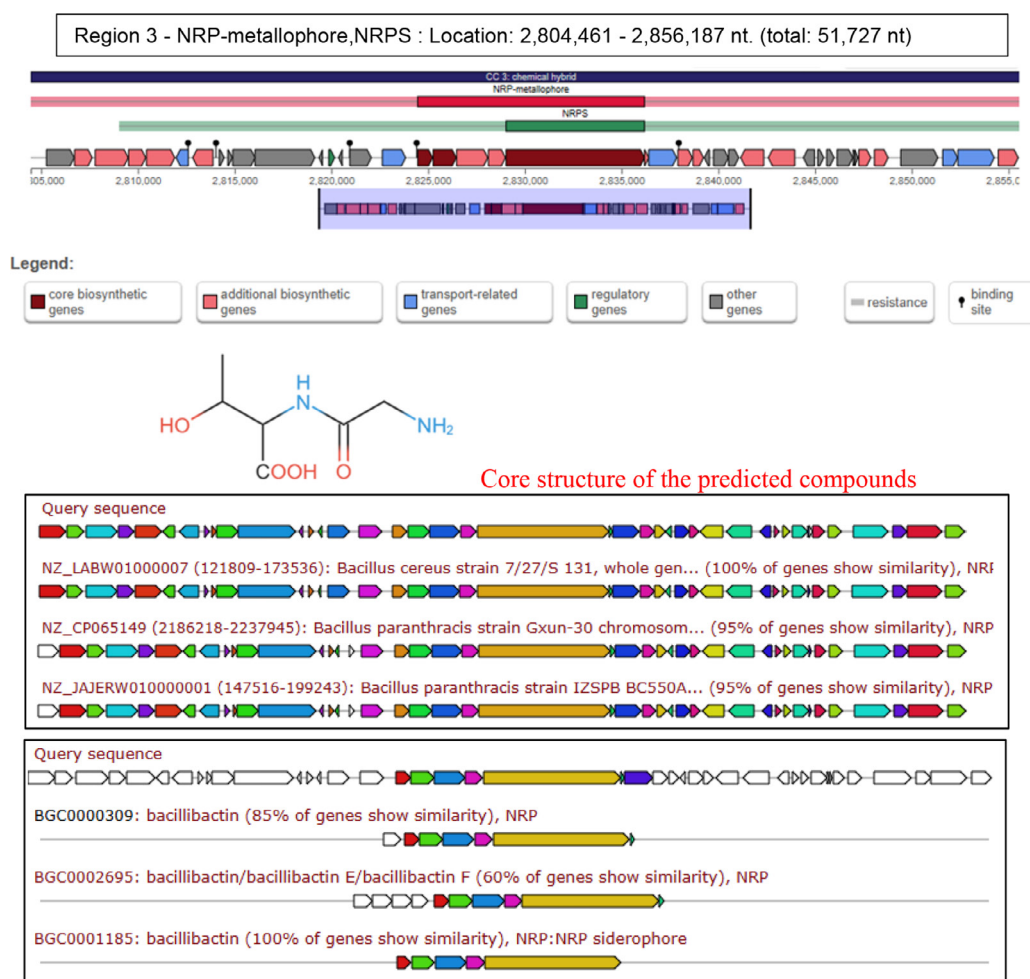


Figure 10. Gene cluster of metallophore compound in *Bacillus paranthracis*. The most similar gene cluster from different bacteria are shown, along with the similarity with known homologous gene clusters involved in the biosynthesis of different metallophore, the related genes are drawn in the same color. The detailed structure of the predicted compound is also displayed (Image produced on antiSMASH)

strains of *Bacillus paranthracis*. Furthermore, the cluster displays varying degrees of similarity with homologous clusters documented in the MIBiG (Minimum Information about a Biosynthetic Gene cluster) database: BGC0000309: Bacillibactin – 85% gene similarity, suggesting strong potential for bacillibactin biosynthesis, albeit with minor variations. BGC0002695: Bacillibactin-related compounds – 60% similarity, indicating lower resemblance and potential structural differences. BGC0001185: Bacillibactin – 100% genetic similarity, confirming perfect identity with a known NRP siderophore cluster. This final cluster strongly suggests that the query genome is capable of producing bacillibactin, a non-ribosomal siderophore involved in iron chelation (Reitz and Medema, 2022). Thus, the antiSMASH results not only validate the isolate's metal-binding potential but also reinforce its environmental adaptability

via secondary metabolite production. The presence of metal-chelating compounds facilitates the uptake of metals from the environment, enabling bacteria to carry out various biological processes, including metal reduction. This reduction can occur through direct or indirect mechanisms. In the direct process, bacteria transfer electrons directly to metal ions such as Fe^{3+} through surface-associated proteins or extracellular structures like cytochrome c. Based on BV-BRC analysis, *Bacillus paranthracis* was found to possess genes encoding cytochrome c, including menaquinone-cytochrome c iron-sulfur reductase. This enzyme functions as an intermediary, transferring electrons from menaquinol to cytochrome c, which subsequently facilitates the reduction of Fe^{3+} to Fe^{2+} . In addition to cytochrome c, genes encoding flavin-containing proteins were also identified, such as NADH:flavin oxidoreductase, NADH

oxidase family proteins, and flavin reductase (EC 1.5.1.30). These flavin-dependent enzymes play a crucial role in Fe^{3+} reduction by transferring electrons via reduced flavin cofactors, such as FMNH₂ and FADH₂, thus contributing to the transformation of Fe^{3+} to Fe^{2+} .

The metallophore produced by *Bacillus paranthracis* is predicted—based on antiSMASH analysis—to be structurally and functionally related to bacillibactin. To further investigate this, the *Bacillus paranthracis* genome was analyzed using BlastKoala (BLASTP Koala) for functional annotation of proteins. Mapping these proteins to metabolic pathways using KEGG (Kyoto Encyclopedia of Genes and Genomes) revealed several enzymes and genes involved in bacillibactin biosynthesis, including [EC: 5.4.4.2], [EC: 3.3.2.1 / 6.3.2.14], [EC: 1.3.1.28], DhbF, DhbE, and DhbB. The biosynthetic pathway for bacillibactin is illustrated in Figure 11.

Bacillibactin is a secondary metabolite secreted by various *Bacillus* species to facilitate iron (Fe^{3+}) acquisition under iron-limited conditions (Chakraborty et al., 2022). The presence of bacillibactin biosynthetic genes in *Bacillus paranthracis* supports its ability to chelate essential metals from the environment, enabling survival and metabolic function in metal-stressed environments. In addition to siderophore production, *Bacillus paranthracis* possesses genes for ATP-Binding Cassette (ABC) transporters, which assist in the active transport of metal ions across the cell membrane. ABC transporters serve dual roles

as importers and exporters (Akhtar and Turner, 2022). Beyond metal ion transport, they are also involved in the uptake of vital nutrients such as sugars, peptides, and amino acids (Zeng and Charkowski, 2021). In this study, the genome of *Bacillus paranthracis* was further examined using BlastKoala to identify ABC transporter genes associated with metal transport. The results of this analysis are presented in Table 5.

Based on KEGG database analysis, further investigation was conducted on the metal transport processes in *Bacillus paranthracis*, specifically focusing on ABC transporter-mediated transmembrane transport. As shown in Table 5, *Bacillus paranthracis* possesses several genes encoding proteins responsible for the uptake of metal ions from the environment. These include: Fe^{3+} -Afu substrate-binding protein (ABC system), Fe^{3+} -dicitrate transport system substrate-binding protein Fec (BCDE), Fe^{3+} -hydroxamate iron complex transporter Fhu (BCD), Fe^{2+} Tro substrate-binding protein (ABCD), Manganese transport system substrate-binding protein Mnt (ABC), Zinc transporter Znu (ABC), Nickel transport system protein Nik (ABCDE). These transport systems collectively contribute to the bacterium's ability to acquire essential metal ions, particularly iron, from its environment. Among them, Afu (ABC), Fec (BCDE), and Fhu (BCD) are key systems for Fe^{3+} uptake, playing critical roles in bacterial iron acquisition. Additionally, the FeuABC transporter gene, responsible for transporting Fe-bacillibactin – a siderophore complex – is present

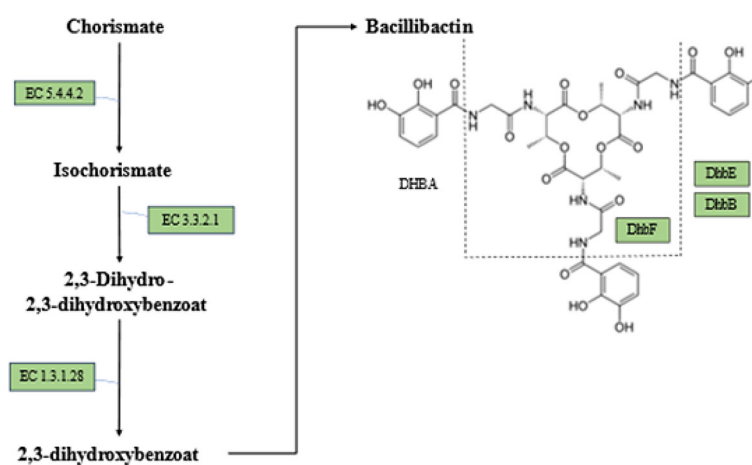


Figure 11. Biosynthesis of bacillibactin from the *Bacillus paranthracis* genome. The results were analyzed using BlastKOALA. salicylate biosynthesis isochorismate synthase [EC: 5.4.4.2], bifunctional isochorismate lyase/aryl carrier protein [EC: 3.3.2.1 / 6.3.2.14], 2,3-dihydro-2,3-dihydroxybenzoate dehydrogenase [EC: 1.3.1.28], DhbF is glycine--[glycyl carrier protein]ligase, DhbE is 2,3-dihydroxybenzoate--[aryl carrier protein]ligase, and DhbB is bifunctional isochorismate carrier protein/aryl carrier protein

Table 5. ABC gene metal transporter in *Bacillus paranthracis*

Substrate	ABC transporter
Fe ³⁺	AfuA, AfuB, AfuC
Fe ³⁺ -dicitrate	FecB, FecC, FecD, FecE
Fe ³⁺ -hydroxamet	FhuD, FhuB, FhuC
Fe ²⁺	TroA, TroC, TroD, TroB
Manganase	MntC, MntB, MntA
Zinc	ZnuA, ZnuB, ZnuC
Nickel	NikA, NikB, NikC, NikD, Nik E
Fe ³⁺ -bacillibactin	FeuA, FeuB, FeuC

in the genome. This complex has been shown to enhance growth in *Bacillus subtilis* (Delepe-laire, 2019), indicating a similar role in *Bacillus paranthracis*.

However, the presence of excess metal ions can induce oxidative stress, leading to cellular damage. To mitigate this, bacteria have developed defense mechanisms, including the MnSOD (Manganese Superoxide Dismutase) and catalase genes, both of which were identified in the *Bacillus paranthracis* genome. MnSOD catalyzes the dismutation of superoxide radicals (O₂⁻) into hydrogen peroxide (H₂O₂) (Gaidamakova et al., 2022), which is subsequently broken down by catalase into water and oxygen (Liu et al., 2025). This antioxidant defense system was supported by experimental evidence: a positive catalase test confirmed the enzymatic activity of catalase in *Bacillus paranthracis* (Figure 6), further validating the presence and functionality of these genes.

CONCLUSIONS

Based on the research conducted, it can be concluded that bacteria capable of reducing iron (Fe) were successfully isolated from red mud waste. The bacterial isolates identified with metal-reducing capabilities include *Kytococcus sedentarius* (As 1), *Staphylococcus arlettae* (As 3), *Halalkalibacterium halodurans* strains (As 6 and As 8), *Bacillus paranthracis* (Ai 3), *Stutzerimonas stutzeri* (Ai 7), and *Cytobacillus firmus* (Ai 8). Among them, *Bacillus paranthracis* (Ai 3) had the highest reduction activity and based on WGS analysis was confirmed to have genes and compounds that are potentially involved in the iron reduction process. These findings highlight the promising potential of these bacterial isolates

as bioremediation agents for addressing environmental pollution, particularly in metal-contaminated areas.

Acknowledgments

We thank to the members of Microbiology Laboratory, Research Center for Biotechnology Universitas Gadjah Mada for all supports and the discussion during the research. We also thank to Integrated Genomic Facility at the Faculty of Biology UGM dor providing Whole Genome Sequencing.

REFERENCES

- Akhtar, A. A., Turner, D. P. (2022). The role of bacterial ATP-binding cassette (ABC) transporters in pathogenesis and virulence: Therapeutic and vaccine potential. *Microbial Pathogenesis*, 171(September 2021), 105734. <https://doi.org/10.1016/j.micpath.2022.105734>
- Algarni, A. A. (2022). Combining of molecular 16S rRNA gene and metabolic fingerprinting through biolog system for the identification of streptomycetes in Saudi Arabia. *Journal of King Saud University - Science*, 34(3), 101889. <https://doi.org/10.1016/j.jksus.2022.101889>
- Aman, I., Maqsood, Q., Mehmood, T., Sumrin, A., Shahzad, R. (2025). Genetic insights and phylogenetic relationships of Momordica balsamina using DNA barcoding: An accurate tool for species identification. *Gene Reports*, 39(March), 102186. <https://doi.org/10.1016/j.genrep.2025.102186>
- Awasti, N., Anand, S. (2022). A fluorescence spectroscopic method for rapid detection of bacterial endospores: Proof of concept. *JDS Communications*, 3(2), 97–100. <https://doi.org/10.3168/jdsc.2021-0170>
- Balamurugan, V., Raja, K., Selvakumar, S., Vasanth, K. (2019). Phytochemical screening, antioxidant, anti-diabetic and cytotoxic activity of leaves of Pandanus canaranus Warb. *Materials Today: Proceedings*, 48, 322–329. <https://doi.org/10.1016/j.matpr.2020.07.603>
- Bilung, L. M., Pui, C. F., Su'Ut, L., Apun, K. (2018). Evaluation of BOX-PCR and ERIC-PCR as Molecular Typing Tools for Pathogenic Leptospira. *Disease Markers*, 2018. <https://doi.org/10.1155/2018/1351634>
- Cain, T. J., Smith, A. T. (2021). Ferric iron reductases and their contribution to unicellular ferrous iron uptake. *Journal of Inorganic Biochemistry*, 218(January), 111407. <https://doi.org/10.1016/j.jinorg.2021.111407>

- jinorgbio.2021.111407
8. Casado-García, Á., Chichón, G., Domínguez, C., García-Domínguez, M., Heras, J., Inés, A., López, M., Mata, E., Pascual, V., Sáenz, Y. (2021). MotilityJ: An open-source tool for the classification and segmentation of bacteria on motility images. *Computers in Biology and Medicine*, 136(May). <https://doi.org/10.1016/j.combiomed.2021.104673>
 9. Chakraborty, K., Kizhakkekalam, V. K., Joy, M., Chakraborty, R. D. (2022). Bacillibactin class of siderophore antibiotics from a marine symbiotic *Bacillus* as promising antibacterial agents. *Applied Microbiology and Biotechnology*, 106(1), 329–340. <https://doi.org/10.1007/s00253-021-11632-0>
 10. Cheng, P., Yang, C., Zhou, S., Huang, J., Liu, R., Yan, B. (2023). Degradation efficiency of antibiotics by the sewage-fed microbial fuel cells depends on gram-staining property of exoelectrogens. *Process Safety and Environmental Protection*, 176(June), 421–429. <https://doi.org/10.1016/j.psep.2023.06.010>
 11. Delepelaire, P. (2019). Bacterial ABC transporters of iron containing compounds. *Research in Microbiology*, 170(8), 345–357. <https://doi.org/10.1016/j.resmic.2019.10.008>
 12. Dong, Y., Zan, J., Lin, H. (2023). Bioleaching of heavy metals from metal tailings utilizing bacteria and fungi: Mechanisms, strengthen measures, and development prospect. *Journal of Environmental Management*, 344(June), 118511. <https://doi.org/10.1016/j.jenvman.2023.118511>
 13. El-Liethy, M. A., Hemdan, B. A., El-Taweel, G. E. (2023). New insights for tracking bacterial community structures in industrial wastewater from textile factories to surface water using phenotypic, 16S rRNA isolates identifications and high-throughput sequencing. *Acta Tropica*, 238(August 2022), 106806. <https://doi.org/10.1016/j.actatropica.2022.106806>
 14. Gaidamakova, E. K., Sharma, A., Matrosova, V. Y., Grichenko, O., Volpe, R. P., Tkavc, R., Conze, I. H., Klimenkova, P., Balygina, I., Horne, W. H., Gostincar, C., Chen, X., Makarova, K. S., Shuryak, I., Srinivasan, C., Jackson-Thompson, B., Hoffman, B. M., Daly, M. J. (2022). Small-Molecule Mn Antioxidants in *Caenorhabditis elegans* and *Deinococcus radiodurans* Supplant MnSOD Enzymes during Aging and Irradiation. *MBio*, 13(1). <https://doi.org/10.1128/MBIO.03394-21>
 15. Ghorbanzadeh, N., Lakzian, A., Haghnia, G. H., Karimi, A. R. (2014). Isolation and identification of ferric reducing bacteria and evaluation of their roles in iron availability in two calcareous soils. *Eurasian Soil Science*, 47(12), 1266–1273. <https://doi.org/10.1134/S1064229314120059>
 16. Giovanella, P., Cabral, L., Costa, A. P., de Oliveira Camargo, F. A., Gianello, C., Bento, F. M. (2017). Metal resistance mechanisms in Gram-negative bacteria and their potential to remove Hg in the presence of other metals. *Ecotoxicology and Environmental Safety*, 140(October 2016), 162–169. <https://doi.org/10.1016/j.ecoenv.2017.02.010>
 17. Gomes, A. F. R., Almeida, M. C., Sousa, E., Resende, D. I. S. P. (2024). Siderophores and metallophores: Metal complexation weapons to fight environmental pollution. *Science of the Total Environment*, 932(May), 173044. <https://doi.org/10.1016/j.scitotenv.2024.173044>
 18. He, Y., Guo, J., Song, Y., Chen, Z., Lu, C., Han, Y., Li, H., Hou, Y., Zhao, R. (2021). Acceleration mechanism of bioavailable Fe(III) on Te(IV) bioreduction of *Shewanella oneidensis* MR-1: Promotion of electron generation, electron transfer and energy level. *Journal of Hazardous Materials*, 403(August 2020). <https://doi.org/10.1016/j.jhazmat.2020.123728>
 19. Hitch, T. C. A., Riedel, T., Oren, A., Overmann, J., Lawley, T. D., Clavel, T. (2021). Automated analysis of genomic sequences facilitates high-throughput and comprehensive description of bacteria. *ISME Communications*, 1(1). <https://doi.org/10.1038/s43705-021-00017-z>
 20. Jing, H., Liu, Z., Chen, J., Ho, C. L. (2022). Elucidation of Iron(III) Bioleaching Properties of Gram-Positive Bacteria. *ACS Omega*, 7(42), 37212–37220. <https://doi.org/10.1021/acsomega.2c03413>
 21. Johnson, J. S., Spakowicz, D. J., Hong, B. Y., Petersen, L. M., Demkowicz, P., Chen, L., Leopold, S. R., Hanson, B. M., Agresta, H. O., Gerstein, M., Sodergren, E., Weinstock, G. M. (2019). Evaluation of 16S rRNA gene sequencing for species and strain-level microbiome analysis. *Nature Communications*, 10(1), 1–11. <https://doi.org/10.1038/s41467-019-13036-1>
 22. Kang, C., Kim, T. (2023). Development of construction materials using red mud and brine. *Case Studies in Construction Materials*, 18(May), e02185. <https://doi.org/10.1016/j.cscm.2023.e02185>
 23. Kappler, A., Bryce, C., Mansor, M., Lueder, U., Byrne, J. M., Swanner, E. D. (2021). An evolving view on biogeochemical cycling of iron. *Nature Reviews Microbiology*, 19(6), 360–374. <https://doi.org/10.1038/s41579-020-00502-7>
 24. Kaur, H., Siddique, R., Rajor, A. (2022). Removal of alkalinity and metal toxicity from incinerated biomedical waste ash by using *Bacillus halodurans*. *Bioremediation Journal*, 26(1), 1–19. <https://doi.org/10.1080/10889868.2021.1884527>
 25. Kee, P. E., Yim, H. S., Kondo, A., Wong, S. Y. W., Chen, P. T., Lan, J. C. W., Ng, H. S. (2021). Incorporation of electric fields to ionic liquids-based aqueous biphasic system for enhanced recovery of extracellular *Kytococcus sedentarius* TWHK01

- keratinase. *Journal of the Taiwan Institute of Chemical Engineers*, 125, 35–40. <https://doi.org/10.1016/j.jtice.2021.06.009>
26. Kislichkina, A. A., Sizova, A. A., Skryabin, Y. P., Dentovskaya, S. V., Anisimov, A. P. (2024). Evaluation of 16S rRNA genes sequences and genome-based analysis for identification of non-pathogenic *Yersinia*. *Frontiers in Microbiology*, 15(January), 1–14. <https://doi.org/10.3389/fmicb.2024.1519733>
27. Kotnala, R. K., Das, R., Shah, J., Sharma, S., Sharma, C., Sharma, P. B. (2022). Red mud industrial waste translated into green electricity production by innovating an ingenious process based on Hydroelectric Cell. *Journal of Environmental Chemical Engineering*, 10(2), 107299. <https://doi.org/10.1016/j.jece.2022.107299>
28. Kunal, Rajor, A., Siddique, R. (2016). Bacterial treatment of alkaline cement kiln dust using *Bacillus halodurans* strain KG1. *Brazilian Journal of Microbiology*, 47(1), 1–9. <https://doi.org/10.1016/j.bjm.2015.11.001>
29. Li, H., Ding, S., Song, W., Zhang, Y., Ding, J., Lu, J. (2022). Iron reduction characteristics and kinetic analysis of *Comamonas testosteroni* Y1: a potential iron-reduction bacteria. *Biochemical Engineering Journal*, 177(October 2021), 108256. <https://doi.org/10.1016/j.bej.2021.108256>
30. Li, Z., Liu, X., Gao, Y., Zhang, J. (2023). Study on the hardening mechanism of Bayer red mud-based geopolymer engineered cementitious composites. *Construction and Building Materials*, 392(April), 131669. <https://doi.org/10.1016/j.conbuildmat.2023.131669>
31. Lim, K. R., Son, J. S., Moon, S. Y. (2021). Case report of infectious spondylitis caused by *kytocos sedentarius*. *Medicina (Lithuania)*, 57(8), 2–5. <https://doi.org/10.3390/medicina57080797>
32. Liu, J., Lu, J., Li, Z., Fan, Y., Liu, S. (2023). An ultra-small fluorescence zero-valent iron nanoclusters selectively kill gram-positive bacteria by promoting reactive oxygen species generation. *Colloids and Surfaces B: Biointerfaces*, 227(February), 113343. <https://doi.org/10.1016/j.colsurfb.2023.113343>
33. Liu, Y., Naidu, R. (2014). Hidden values in bauxite residue (red mud): Recovery of metals. *Waste Management*, 34(12), 2662–2673. <https://doi.org/10.1016/j.wasman.2014.09.003>
34. Liu, Z., Lei, L., Zhang, Z., Du, M., Chen, Z. (2025). Ultrasound-responsive engineered bacteria mediated specific controlled expression of catalase and efficient radiotherapy. *Materials Today Bio*, 31(December 2024), 101620. <https://doi.org/10.1016/j.mtbio.2025.101620>
35. Luo, Z., Su, J., Luo, S., Ju, Y., Chen, B., Gu, Q., Zhou, H. (2024). Structure-guided inhibitor design targeting CntL provides the first chemical validation of the staphylopine metallophore system in bacterial metal acquisition. *European Journal of Medicinal Chemistry*, 280(October). <https://doi.org/10.1016/j.ejmech.2024.116991>
36. Madhaiyan, M., Saravanan, V. S., See-Too, W.-S. (2020). Genome based analyses reveals the presence of heterotypic synonyms and subspecies in bacteria and archaea. *BioRxiv*. <https://doi.org/10.1101/2020.12.13.418756>
37. Man, Y., Zhang, H., Huang, J., Xi, S., Wang, J., Tao, H., Zhou, Y. (2022). Combined effect of tetracycline and copper ion on catalase activity of microorganisms during the biological phosphorus removal. *Journal of Environmental Management*, 304(December 2021), 114218. <https://doi.org/10.1016/j.jenvman.2021.114218>
38. Mandal, A. K., Sen, R. (2018). Preservation of higher Fe[II] content in borosilicate glass by microwave irradiation in air. *Materials Research Bulletin*, 108(May), 156–162. <https://doi.org/10.1016/j.materresbull.2018.08.034>
39. Mathivanan, K., Chandirika, J. U., Vinothkanna, A., Yin, H., Liu, X., Meng, D. (2021). Bacterial adaptive strategies to cope with metal toxicity in the contaminated environment – A review. *Ecotoxicology and Environmental Safety*, 226, 112863. <https://doi.org/10.1016/j.ecoenv.2021.112863>
40. Matus, F., Stock, S., Eschenbach, W., Dyckmans, J., Merino, C., Nájera, F., Köster, M., Kuzyakov, Y., Dippold, M. A. (2019). Ferrous Wheel Hypothesis: Abiotic nitrate incorporation into dissolved organic matter. *Geochimica et Cosmochimica Acta*, 245, 514–524. <https://doi.org/10.1016/j.gca.2018.11.020>
41. Nakamiya, K., Nakayama, T., Ito, H., Edmonds, J. S., Shibata, Y., Morita, M. (2007). Degradation of arylarsenic compounds by microorganisms. *FEMS Microbiology Letters*, 274(2), 184–188. <https://doi.org/10.1111/j.1574-6968.2007.00835.x>
42. Newell, P. D., Fricker, A. D., Roco, C. A., Chandrangsu, P., Merkel, S. M. (2013). A Small-Group Activity Introducing the Use and Interpretation of BLAST. *Journal of Microbiology & Biology Education*, 14(2), 238–243. <https://doi.org/10.1128/jmbe.v14i2.637>
43. Nikolić, I., Stanković, S., Dimkić, I., Berić, T., Stojšin, V., Janse, J., Popović, T. (2018). Genetic diversity and pathogenicity of *Pseudomonas syringae* pv. aptata isolated from sugar beet. *Plant Pathology*, 67(5), 1194–1207. <https://doi.org/10.1111/ppa.12831>
44. Poonchareon, K., Pulsrikarn, C., Nuanmuang, N., Khamai, P. (2019). Effectiveness of BOX-PCR in differentiating genetic relatedness among *Salmonella enterica* Serotype 4,[5],12:i:- Isolates from hospitalized patients and minced pork samples in Northern Thailand. *International Journal of Microbiology*,

2019. <https://doi.org/10.1155/2019/5086240>
45. Rao, K., Narasu, M. L. (2007). Alkaline protease from *Bacillus firmus* 7728. *African Journal of Biotechnology*, 6(21), 2493–2496. <https://doi.org/10.5897/ajb2007.000-2395>
 46. Reddy, N. G., Rao, B. H. (2018). Compaction and consolidation behaviour of untreated and treated waste of Indian red mud. *Geotechnical Research*, 5(2), 106–121. <https://doi.org/10.1680/jgere.18.00005>
 47. Reitz, Z. L., Medema, M. H. (2022). Genome mining strategies for metallophore discovery. *Current Opinion in Biotechnology*, 77(Iii), 102757. <https://doi.org/10.1016/j.copbio.2022.102757>
 48. Rossi-Tamisier, M., Benamar, S., Raoult, D., Fournier, P. E. (2015). Cautionary tale of using 16s rRNA gene sequence similarity values in identification of human-associated bacterial species. *International Journal of Systematic and Evolutionary Microbiology*, 65(6), 1929–1934. <https://doi.org/10.1099/ijs.0.000161>
 49. Sagar, S., Dwivedi, A., Yadav, S., Tripathi, M., Kaistha, S. D. (2012). Chemosphere Hexavalent chromium reduction and plant growth promotion by *Staphylococcus arlettae* Strain Cr11. *Chemosphere*, 86(8), 847–852. <https://doi.org/10.1016/j.chemosphere.2011.11.031>
 50. Sarath Chandra, K., Krishnaiah, S. (2022). Strength and leaching characteristics of red mud (bauxite residue) as a geomaterial in synergy with fly ash and gypsum. *Transportation Research Interdisciplinary Perspectives*, 13, 100566. <https://doi.org/10.1016/j.trip.2022.100566>
 51. Sathishkumar, K., Murugan, K., Benelli, G., Higuchi, A., Rajasekar, A. (2017). Bioreduction of hexavalent chromium by *Pseudomonas stutzeri* L1 and *Acinetobacter baumannii* L2. *Annals of Microbiology*, 67(1), 91–98. <https://doi.org/10.1007/s13213-016-1240-4>
 52. Sau, G. B., Chatterjee, S., Mukherjee, S. K. (2010). Chromate reduction by cell-free extract of *Bacillus firmus* KUCr1. *Polish Journal of Microbiology*, 59(3), 185–190. <https://doi.org/10.33073/pjm-2010-029>
 53. Sazykin, I. S., Sazykina, M. A. (2023). The role of oxidative stress in genome destabilization and adaptive evolution of bacteria. *Gene*, 857(January), 147170. <https://doi.org/10.1016/j.gene.2023.147170>
 54. Schalk, F., Gostincar, C., Kreuzenbeck, N. B., Conlon, B. H., Sommerwerk, E., Rabe, P., Burkhardt, I., Krüger, T., Kniemeyer, O., Brakhage, A. A., Gunde-Cimerman, N., de Beer, Z. W., Dickschat, J. S., Poulsen, M., Beemelmans, C. (2021). The termite fungal cultivar *Termitomyces* combines diverse enzymes and oxidative reactions for plant biomass conversion. *MBio*, 12(3). <https://doi.org/10.1128/mBio.03551-20>
 55. Sims, D., Brettin, T., Detter, J. C., Han, C., Lapidus, A., Copeland, A., del Rio, T. G., Nolan, M., Chen, F., Lucas, S., Tice, H., Cheng, J. F., Bruce, D., Goodwin, L., Pitluck, S., Ovchinnikova, G., Pati, A., Ivanova, N., Mavromatis, K., ... Klenk, H. P. (2009). Complete genome sequence of *Kytococcus sedentarius* type strain (541 T). *Standards in Genomic Sciences*, 1(1), 12–20. <https://doi.org/10.4056/sigs.761>
 56. Smith, G. L., Reutovich, A. A., Srivastava, A. K., Reichard, R. E., Welsh, C. H., Melman, A., Bou-Abdallah, F. (2021). Complexation of ferrous ions by ferrozine, 2,2'-bipyridine and 1,10-phenanthroline: Implication for the quantification of iron in biological systems. *Journal of Inorganic Biochemistry*, 220(April), 111460. <https://doi.org/10.1016/j.jinorgbio.2021.111460>
 57. Sousa, A. M., Machado, I., Nicolau, A., Pereira, M. O. (2013). Improvements on colony morphology identification towards bacterial profiling. *Journal of Microbiological Methods*, 95(3), 327–335. <https://doi.org/10.1016/j.mimet.2013.09.020>
 58. Spinler, J. K., Raza, S., Thapa, S., Venkatachalam, A., Scott, T., Runge, J. K., Dunn, J., Versalovic, J., Luna, R. A. (2022). Comparison of whole genome sequencing and repetitive element PCR for multi-drug-resistant *Pseudomonas aeruginosa* strain typing. *Journal of Molecular Diagnostics*, 24(2), 158–166. <https://doi.org/10.1016/j.jmoldx.2021.10.004>
 59. Vigneshwaran, S., Uthayakumar, M., Arumugaprabu, V. (2020). Potential use of industrial waste-red mud in developing hybrid composites: A waste management approach. *Journal of Cleaner Production*, 276, 124278. <https://doi.org/10.1016/j.jclepro.2020.124278>
 60. Viljoen, C. D., Booysen, C., Sreenivasan Tantuan, S. (2022). The suitability of using spectrophotometry to determine the concentration and purity of DNA extracted from processed food matrices. *Journal of Food Composition and Analysis*, 112(June). <https://doi.org/10.1016/j.jfca.2022.104689>
 61. Yao, Y., Wang, L., Hemamali Peduruhewa, J., Van Zwieten, L., Gong, L., Tan, B., Zhang, G. (2023). The coupling between iron and carbon and iron reducing bacteria control carbon sequestration in paddy soils. *Catena*, 223(January), 106937. <https://doi.org/10.1016/j.catena.2023.106937>
 62. Yuan, F., Yin, S., Xu, Y., Xiang, L., Wang, H., Li, Z., Fan, K., Pan, G. (2021). The richness and diversity of catalases in bacteria. *Frontiers in Microbiology*, 12(March), 1–11. <https://doi.org/10.3389/fmicb.2021.645477>
 63. Zeng, Y., Charkowski, A. O. (2021). The role of ATP-binding cassette transporters in bacterial phytopathogenesis. *Phytopathology*, 111(4), 600–610. <https://doi.org/10.1094/PHYTO-06-20-0212-RVW>